Turkish Journal of Electrical Engineering & Computer Sciences

http://journals.tubitak.gov.tr/elektrik/

Research Article

Turk J Elec Eng & Comp Sci
(2016) 24: 3759 – 3768

doi:10.3906/elk-1412-15

The phononic crystal interface layer determines slow-wave and pulse broadening effects

Li SUN, Aiming JI, Jialing HU, Canyan ZHU, Lijun ZHANG, Jianfeng YANG, Ling-Feng MAO*
Institute of Intelligent Structure and System, Soochow University, Suzhou, P.R. China

Received: 04.12.2014 • **Accepted/Published Online:** 11.06.2015 • **Final Version:** 20.06.2016

Abstract: The relationship among the slow-wave and echo pulse broadening effects in reflected acoustic waves and the width of the interface layer of phononic crystal has been theoretically investigated. It has been observed that not only the slow time for the reflected acoustic wave but also the echo pulse broadening reaches a saturation point as the size of the phononic crystal increases. From the viewpoint of the acoustic wave, there is an interface layer in the crystal that determines the slow-wave and the echo pulse broadening effects. The longest slow time, which is the time needed for transmitting 0.08 periods of the phononic crystal, occurs when the width of the interface layer is $1.89\,\lambda$. The width of the echo pulse is broadened no more than 0.13 periods when the interface layer width is about $2.69\,\lambda$.

Key words: Phononic crystal interface layer, slow-wave effect, echo pulse broadening, finite-difference time-domain simulation

1. Introduction

The propagation of acoustic waves can be guided, controlled, and manipulated by using phononic crystals [1]. Phononic crystals are artificially formed of periodic composite materials or from the periodical distribution of scatterers of acoustic waves (they are mutually disconnected materials in the substrate materials) in a matrix [2]. In recent years, the study of the transmission coefficient, the dispersion relations, and the dynamics of the wave fields by analyzing the transmission spectra in phononic crystals has attracted considerable attention. More researchers have focused on the slow acoustic wave modes with the aim of designing delay lines, filters, and resonators [3,4]. The slow-wave effects in phononic crystals can be studied through analyzing the characteristics of the echo pulse [5]. It can be noted that researchers have paid more attention to the ability to slow the velocity of sound with phononic crystals, which is called the slow-wave effect.

Wave propagation in media obeys a known dispersion relation. The group velocity $v_g = d\omega(k)/dk$ is the speed of a pulse or signal [6]. When an acoustic wave propagates in a phononic crystal, the resonance of acoustic waves caused by scatterers can lead to considerable frequency dispersion and thus substantially reduce the group velocity. The scatterers have a large impact on the transmitted acoustic wave, but the transmitted wave maintains temporal and spatial coherence with the incident pulse [7]. Usually, most works focus on the sound velocity travelling through the phononic crystals for the transmitted wave [8,9]. Therefore, this paper devotes its efforts to discussing the slow-wave effect from a new aspect by analyzing the reflected wave. An interface is defined as a surface that can be treated as the common boundary between 2 different materials [10,11]. The properties of the interface depend on the type of the system. The interface layer in the phononic

*Correspondence: lingfengmao@suda.edu.cn

crystal may lead to various phenomena in the propagation of acoustic waves [12]. On the other hand, the width of the interface layer is an important factor in determining the performance of the interface layer. Therefore, this paper focuses on how the interface layer in the phononic crystal influences the slow-wave effect and the echo pulse broadening phenomenon by analyzing the echo signal in the time domain.

To achieve the goal of the paper, we calculate the propagation of the acoustic wave traveling in the phononic crystals by using finite-difference time-domain (FDTD) simulation software. The FDTD method solves the elastic wave equations via discretizing time and space and replacing derivatives by finite differences in the equations of motion. The FDTD method has been used extensively to study the propagation of electromagnetic waves [13,14] and has also been extended to study phononic crystals [15–18].

2. Theory

The transmission characteristics of acoustic waves in different media are distinct according to the elastodynamic theory. The elastodynamic equations for an isotropic solid medium can be written as:

$$(\lambda+2\mu)\,\nabla\nabla u-\mu\nabla\times\nabla\times u=\rho\frac{\partial^2 u}{\partial t^2} \tag{1}$$

where u is the particle displacement, $\rho$is the mass density, E is Young's modulus, G is the shear modulus, and $\lambda$and μ are Lame constants ($\lambda=\frac{G(E-2G)}{3G-E}$ and $\mu=G$). The elastodynamic equation for a fluid medium can be written as:

$$\frac{1}{c}\frac{\partial^2 p}{\partial t^2}-\nabla^2 p=0 \tag{2}$$

where c is the compressional velocity, and p is the sound pressure.

In this paper, the simulation of ultrasound propagation in the phononic crystal is performed using SimSonic2D, which is based on the FDTD method for solving the elastodynamic equations [19]. The computations in SimSonic2D are based on the following elastodynamic equations:

$$\rho\,(X)\,\frac{\partial v_i}{\partial t}\,(X,t)=\sum_{j=1}^{d}\frac{\partial T_{ij}}{\partial x_{ij}}\,(X,t)+f_i(X,t) \tag{3}$$

$$\frac{\partial T_{ij}}{\partial x_t}\,(X,t)=\sum_{j=1}^{d}\sum_{i=1}^{d}c_{ijkl}(X)\frac{\partial v_k}{\partial x_l}(X,t)+\theta_{ij}(X,t) \tag{4}$$

where $\rho\,(X)$ is the mass density, $c(X)$ is the fourth-order rigidity tensor, and$X$ and t are the space and time variables, respectively. The material properties and geometry of the considered media can be defined by using these parameters. Eqs. (3) and (4) describe the acoustic waves' propagation in the continuous media, which obeys Hooke's law.

The development of phononic crystals for the purpose of controlling acoustic waves has followed the analogous concept of photonic crystals for electromagnetic waves [20–22]. Slow light effect is also one of the greatest properties of photonic crystals [23]. The group velocity can be determined by inversing the first-order dispersion [24]:

$$v_g=\left(\frac{dk}{d\omega}\right)^{-1} \tag{5}$$

where ω and k are frequency and wave vector, respectively. The phase velocity is:

$$v_p = \frac{\omega}{k} = \frac{c}{n} \tag{6}$$

where c is the speed of light in vacuum, and n is the refractive index, which is correlated with ω, $n = n(\omega)$. Thus, the group velocity is:

$$v_g = \frac{c}{n(\omega) + \omega \frac{dn(\omega)}{d\omega}} \tag{7}$$

If $dn(\omega)/d\omega > 0$, then $v_g < v_p$, which represents the light, is slowed in photonic crystals. Compared to the light, the phase velocity and the group velocity of the acoustic wave are defined as follows:

$$v_p = \frac{dx}{dt} = \frac{\omega}{k} = f\lambda \tag{8}$$

$$v_g = \frac{d\omega}{dk} = \frac{d(v_p k)}{dk} = v_p + k\frac{dv_p}{dk} = v_p + \frac{2\pi}{\lambda}\frac{dv_p}{d\frac{2\pi}{\lambda}} = v_p - \lambda\frac{dv_p}{d\lambda} \tag{9}$$

It comes to the conclusion that the speed of the acoustic wave can be slowed down in phononic crystals if$dv_p/d\lambda > 0$.

3. Numerical results and discussion

The calculations in this paper are based on a 2-dimensional phononic crystal. Aluminum is the most abundant metal in the earth's crust and it is the third most abundant element on earth. Structures made from aluminum and its alloys are vital to the aerospace industry [25]. The simulation structure in this paper is set as a thin aluminum plate, inside which are some holes arranged as a square array. These holes are filled with water. Thus, the simulation material consists of aluminum and water.

Perfectly matched layers (PMLs) [26,27] are defined in the simulation frontiers. A PML in SimSonic2D can be expressed as a coefficient of reflection. In practice, the maximum efficiency of a PML depends on the thickness of the PML relative to the wavelength of the incident wave. As a rule of thumb, a PML should have a thickness of at least 1 wavelength in order to get an efficiency of several tens of dB for normal incidence [28]. Here the thickness of the PML is 2 wavelengths.

The simulation system block diagram is illustrated in Figure 1. The side length of the square aluminum plate is 50 mm. During the FDTD simulation, the spatial grid step in x and y dimensions are both 0.02 mm and the time step is 2.22 ns to ensure computational accuracy. The geometry of the source object is a line array. The length of the source array is 8 mm. The incident wave is in the form of normal incidence. The source signal is the continuous sinusoidal ultrasonic signal in the form of:

$$s(t) = \sin(2\pi f_0 t) \tag{10}$$

where f_0 is the frequency of the ultrasonic signal. The frequency is set as 1 MHz in the simulation. The signal duration is 500 ns, so it can be considered as a pulse signal. The speed of ultrasound depends strongly on the temperature. With the increase of the temperature, the speed grows accordingly. In water, the velocity obtained at 25 ° C is about 1497 m/s and for 74 ° C it is 1555 m/s [29]. The velocity in aluminum is 6350 ± 230 m/s when the temperature is 25 ° C [30]. In theoretical computation, the simulation is conducted at

room temperature (25 ° C). In this paper, the speed of ultrasound in aluminum and water is set as 6325 m/s and 1500 m/s, respectively. Thus, the wavelength of the ultrasound in aluminum is 6.325 mm. The receiver for detecting signals occupies 1 grid. The receiver is located at 1.6 mm from the left side of the plate, as shown in Figure 1.

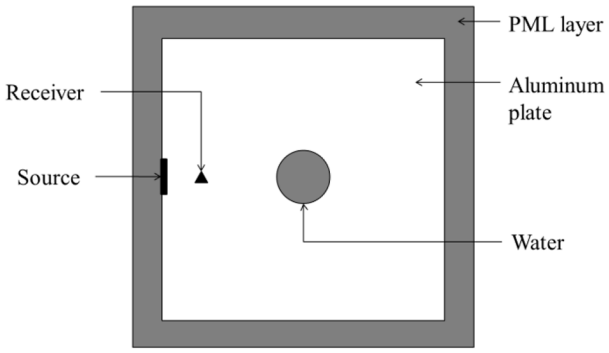

Figure 1. Simulation system block diagram.

In order to explore how the width of the phononic crystal interface layer affects the slow-wave effect and the echo pulse broadening effect, the holes are arranged as a $n \times n$ matrix, and n (the matrix index) is increased to obtain different structures. For different ns, the first columns of holes from the left are all placed along the center line of the plate as shown in Figure 2. The 1×1, 2×2, 3×3, and 6×6 structures are depicted in Figures 2a–2d, respectively. The diameter of the holes d and the lattice constant a are illustrated in Figure 2e. In the calculations, 2 different lattice constants are considered: $a = 0.7$ mm and $a = 1.875$ mm. The diameters of holes are $d = 0.625$ mm and $d = 1.5625$ mm accordingly. For $a = 0.7$ mm, the matrix index n increases to 28 at most. For $a = 1.875$ mm, n increases to 14 at most in order to guarantee that the holes still stay inside the aluminum plate. Meanwhile, the side length (*Length*) of the interface shown in Figure 2d can be simply calculated as follows:

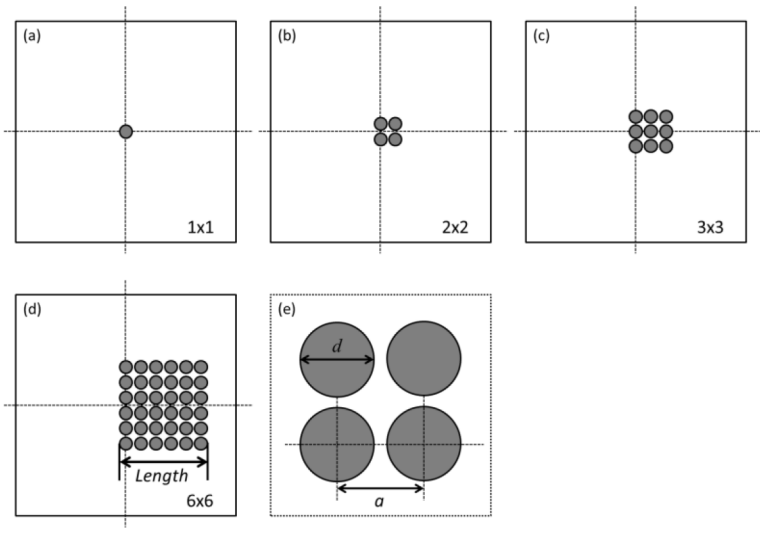

Figure 2. Diagrammatic sketch of the structure of the aluminum plate (a is the lattice constant and d is the diameter of the hole (the scatterer)).

$$Length = d + (n-1) * a \tag{11}$$

In this case, the same width of the interface layer consists of 2 different lattice constants. Under both circumstances, the effect of the interface layer can be observed contrastively.

First the simulation is conducted with $a = 0.7$ mm, $d = 0.625$ mm. In this condition, the diameter of the holes is about one-tenth of the acoustic wavelength. Figure 3 shows the time-domain transmitted ultrasonic signal for different structures of the aluminum plate detected by the receiver. The simulation time is set as 50 mu s. Figure 3a represents the time-domain waveform for the whole simulation time. Because the receiver is set between the signal and the holes, the first positive pulse is the incident wave and the second negative pulse is the reflected echo according to the comparison of the red curve and the blue one. Between these 2 pulses, the receiver does not get any signal because the receiver has detected the incident signal and has not received the echo signal reflected back from the holes. The red curve is the reference curve, indicating that the signal transmits through the plate without meeting any holes. In order to examine the echo in detail, the echo curve is amplified and results for different structures are depicted together for comparison as shown in Figure 3b.

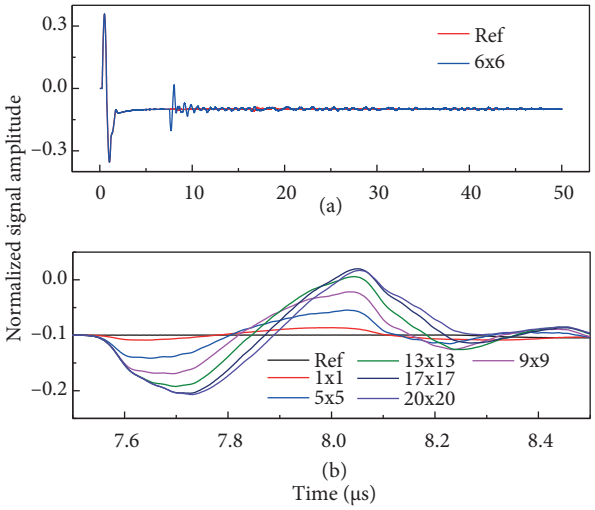

Figure 3. Time-domain transmitted ultrasonic signal for different structures of the aluminum plate, where Ref represents the plate without the hole.

Figure 4 demonstrates the arrival time of the amplitude of the negative pulse with different structures when $a = 0.7$ mm. It is obvious that the arrival time increases as matrix index n rises. However, from $n = 17$, the arrival time tends to saturate. Notice that when $n = 17$, the side length of the matrix ($Length = 11.825$ mm) is equivalent to 1.87λ ($\lambda = 6.325$ mm). Therefore, the conclusion can be drawn that the largest width of the interface layer is $1.87\lambda$for the slow wave.

In order to observe the slow-wave effect in different structures, 2 parameters, "number of periods" and "relative change", are defined. Number of periods is computed by the following formula:

$$N = (T_n - T_1)/T, n = 1, 2, 3, ... \tag{12}$$

Relative change is calculated as:

$$R = (T_n - T_1)/T_1 * 100\%, n = 1, 2, 3, ... \tag{13}$$

where N is the number of periods, R is the relative change, T is the period of incident acoustic wave, and T_n is the arrival time of the lowest amplitude of the echo signal for holes array index n. For example, T_1 is the echo arrival time for $n = 1$.

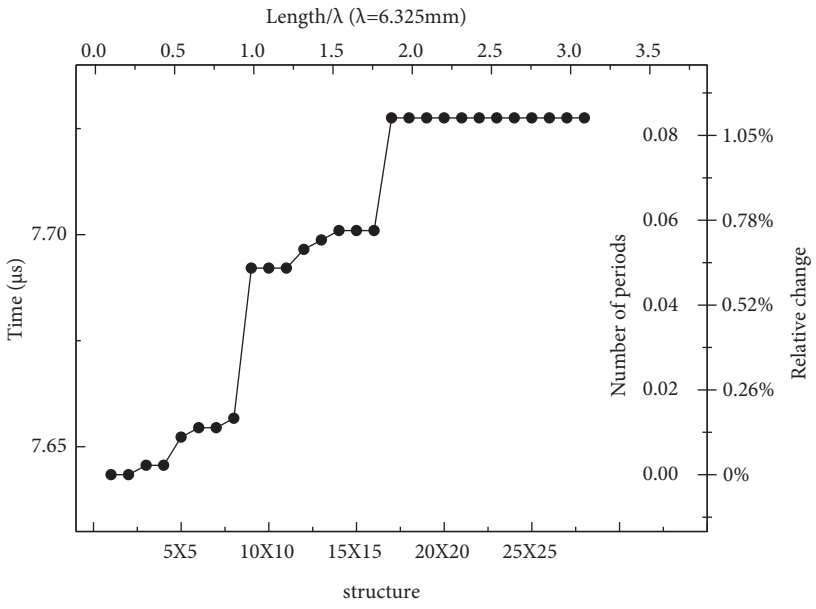

Figure 4. The arrival time of the lowest amplitude of the echo signal for different structures ($a = 0.7$ mm and $d = 0.625$ mm).

The intersection time is defined as the point where the rising part of the echo signal intersects with the reference curve. Figure 5 shows the intersection time of the echo signal for different structures when the diameter of the holes is 0.625 mm. The curve generally rises as n increases. The side length of the structure for $n = 25$ ($Length = 17.425$ mm) is equivalent to 2.75λ ($\lambda = 6.325$ mm), where the intersection time reaches the maximum. As n continues to increase, the curve tends to saturate. The width of the echo pulse is broadened when *Length* increases. When *Length* is larger than 17.425 mm, the broadening effect becomes steady and so the width of the interface layer is 1.87λ for echo pulse broadening. The number of periods and relative change are calculated by Eqs. (12) and (13), respectively.

In this paper, the simulation is conducted for 2 different sizes: (i) $a = 0.7$ mm, $d = 0.625$ mm, and (ii) $a = 1.875$ mm, $d = 1.5625$ mm. The arrival times of the lowest amplitude of the echo signal for the 2 cases are shown in Figures 6a and 6b, respectively. Some similarities can be drawn from the 2 curves. First, the time rises as *Length* increases. Second, when *Length* reaches about 12 mm, which is equivalent to 1.89λ ($\lambda = 6.325$ mm), both curves tend to saturate. It is indicated that the echo pulse is slowed for about 0.08 periods (1.05%) at most for size (i) and about 0.07 periods (0.93%) for size (ii). It is worth noticing that when *Length* reaches a certain value (1.89λ in this frequency), the change trend of the slow-wave effect is the same for these 2 sizes. That is to say, when the frequency in the simulation does not change, no matter what sizes the lattice constants and the diameters are, the width of the phononic crystal interface layer is determined, here as 1.89λ. When *Length* is equal to the width of the interface layer, the slow-wave effect will be the best, and even if *Length* continues to increase, the effect will not change as long as *Length* is larger than the width of the interface layer.

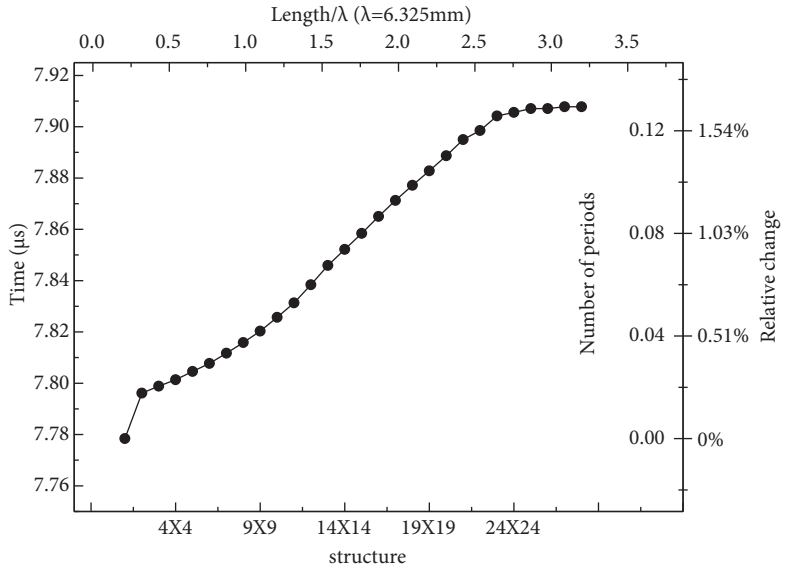

Figure 5. The intersection time of the echo signal for different structures ($a = 0.7$ mm and $d = 0.625$ mm).

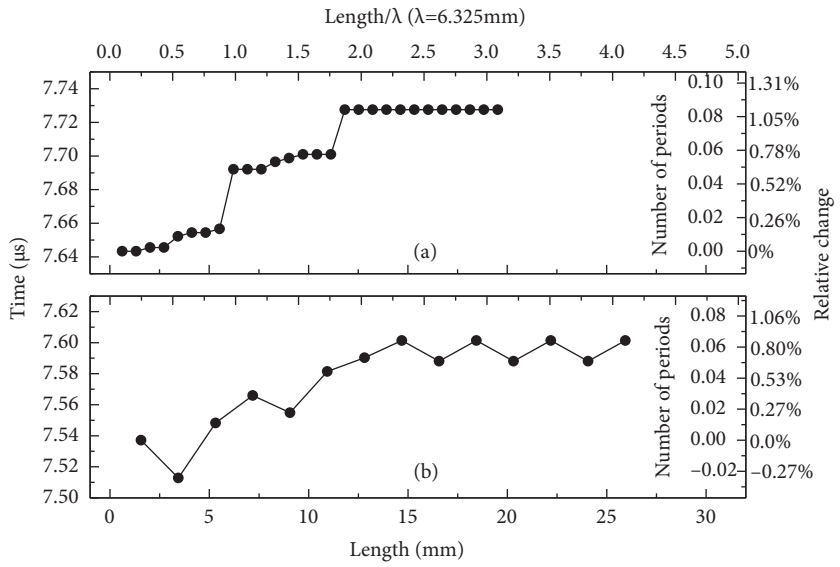

Figure 6. The arrival time of the lowest amplitude of the echo signal for different structures: (a) $a = 0.7$ mm and $d = 0.625$ mm, (b) $a = 1.875$ mm and $d = 1.5625$ mm.

Figures 7a and 7b demonstrates the intersection time of the echo signal for the 2 structures ((i) $a = 0.7$ mm, $d = 0.625$ mm, (ii) $a = 1.875$ mm, $d = 1.5625$ mm). The arrival time of the lowest amplitude of the echo signal rises as *Length* increases. When *Length* is about 17 mm, which is equivalent to 2.69λ ($\lambda = 6.325$ mm), the 2 curves tend to saturate. It is obvious that the width of the echo pulse is broadened for about 0.13 periods (1.67%) at most for the former condition and about 0.1 (1.3%) periods for the latter. Accordingly, when the length of the interface is about 2.69λ, the pulse broadening effect caused by the phononic crystal will stay the same. In other words, under a certain frequency, no matter what sizes the lattice constants and the diameters are, there is always an interface layer that keeps the broadening effect confined to a certain level.

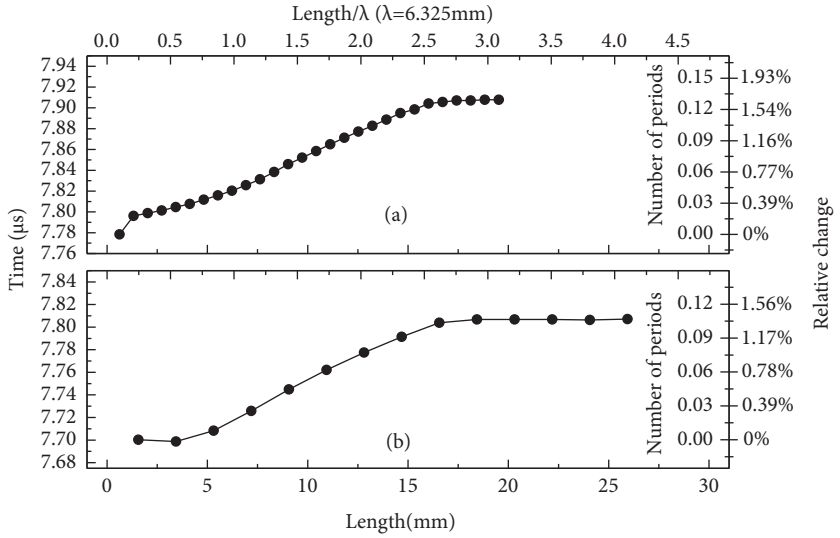

Figure 7. The intersection time of the echo signal for different structures: (a) $a = 0.7$ mm and $d = 0.625$ mm, (b) $a = 1.875$ mm and $d = 1.5625$ mm.

4. Conclusions

In this paper, the impacts of the interface layer in the phononic crystal on the slow-wave effect and the echo pulse broadening have been theoretically investigated using FDTD simulations. By studying the time-domain waveform while *Length* is not larger than the width of the interface layer it can be seen that, for the 2 different crystal structures, the arrival time of the echo signal is slowed and the width of the echo pulse is broadened when the size of the structure increases. However, when the diameters and lattice constants are smaller, the slow-wave effect and the echo pulse broadening phenomenon will be obvious. For the smaller size, the echo pulse is slowed down for about the time that is needed for transmitting 0.08 periods (1.05%) of phononic structure at most. Similarly, the width of the echo pulse is broadened for about 0.13 periods (1.67%) at most. If the size of the structure continues to increase, these 2 parameters tend to saturate. It can be concluded that the change in both parameters will be limited to a certain range if the frequency of the incident acoustic pulse is fixed. That is to say, there is an interface layer in the crystal from the viewpoint of the acoustic wave and this interface layer determines the slow-wave effect and the echo pulse broadening effect. Thus, the degrees of the slow-wave effect and the echo pulse broadening effect are influenced by changing the sizes of the lattice constants and the diameters. The interface layer in the phononic crystal is a crucial factor in deciding whether there are these effects or not. This work is helpful in understanding the control of acoustic-wave propagation in phononic crystals. Specifically, if the sound velocity is slowed down or the echo pulse width is broadened by adding a phononic crystal into the structure, then more attention must be paid to the interface layer in the phononic crystal. When the crystal size increases the interface layer size, the slow-wave effect and the pulse broadening effect will saturate. That is, if better slow-wave or echo pulse broadening effects are wanted, it will make no sense to increase the phononic crystal size continuously. The theoretical results in this paper can lay a good foundation for understanding the slowing effects of the interface layer in engineering applications. They can provide many potential applications in acoustic waveform regulation, velocity control, and the design of new acoustic devices.

Acknowledgments

The authors acknowledge assistance and support from the National Natural Science Foundation of China under Grant Nos. 61076102 and 61272105, and the Natural Science Foundation of Jiangsu Province of China under Grant No. BK2012614.

References

[1] Amoudache S, Pennec Y, Rouhani BD, Khater A, Lucklum R, Tigrine R. Simultaneous sensing of light and sound velocities of fluids in a two-dimensional phoXonic crystal with defects. J Appl Phys 2014; 115: 134503.

[2] Wu TT, Huang ZG, Lin S. Surface and bulk acoustic waves in two-dimensional phononic crystal consisting of materials with general anisotropy. Phys Rev B 2004; 69: 094301.

[3] Zhang X, An ZW. Numerical investigation of the slow acoustic wave modes in a one-dimensional phononic crystal plate. Chinese Phys Lett 2013; 30: 086301.

[4] Huang CY, Sun JH, Wu TT. A two-port ZnO/silicon Lamb wave resonator using phononic crystals. Appl Phys Lett 2010; 97: 031913.

[5] Liu J, Li F, Wu YH. The slow zero order antisymmetric Lamb mode in phononic crystal plates. Ultrasonics 2013; 53: 849-852.

[6] Page JH, Sheng P, Schriemer HP, Jones I, Jing XD, Weitz DA. Group velocity in strongly scattering media. Science 1996; 271: 634-637.

[7] Page JH, Schriemer HP, Jones I, Sheng P, Weitz DA. Classical wave propagation in strongly scattering media. Physica A 1997; 241: 64-71.

[8] Page JH, Yang SX, Liu ZY, Cowan ML, Chan CT, Sheng P. Tunneling and dispersion in 3D phononic crystals. Z Kristallogr 2005; 220: 859-870.

[9] Bonello B, Charles C, Ganot F. Velocity of a SAW propagating in a 2D phononic crystal. Ultrasonics 2006; 44: 1259-1263.

[10] Sommer FG, Filly RA, Minton MJ. Acoustic shadowing due to refractive and reflective effects. Am J Roentgenol 1979;132: 973-979.

[11] Myers D. Surfaces, Interfaces and Colloids. 2nd ed. New York, NY, USA: Wiley, 1990.

[12] Friedrichs KO, Keller JB. Geometrical acoustics. II. Diffraction, reflection, and refraction of a weak spherical or cylindrical shock at a plane interface. J Appl Phys 1955; 26: 961-966.

[13] Cangellaris AC, Wright DB. Analysis of the numerical error caused by the stair-stepped approximation of a conducting boundary in FDTD simulations of electromagnetic phenomena. IEEE T Antenn Propag 1991; 39: 1518-1525.

[14] Sui W, Christensen DA, Durney CH. Extending the two-dimensional FDTD method to hybrid electromagnetic systems with active and passive lumped elements. IEEE T Microw Theory 1992; 40: 724-730.

[15] Lambin P, Khelif A, Vasseur JO, Dobrzynski L, Djafari-Rouhani B. Stopping of acoustic waves by sonic polymer-fluid composites. Phys Rev E 2001; 63: 066605.

[16] Chandra H, Deymier P A, Vasseur J O. Elastic wave propagation along waveguides in three-dimensional phononic crystals. Phys Rev E 2004; 70: 054302.

[17] Vasseur JO, Deymier PA, Chenni B, Djafari-Rouhani B, Dobrzynski L, Prevost D. Experimental and theoretical evidence for the existence of absolute acoustic band gaps in two-dimensional solid phononic crystals. Phys Rev Lett 2001; 86: 3012.

[18] Tanaka Y, Tomoyasu Y, Tamura S. Band structure of acoustic waves in phononic lattices: two-dimensional composites with large acoustic mismatch. Phys Rev B 2000; 62: 7387.

[19] Bossy E, Talmant M, Laugier P. Three-dimensional simulations of ultrasonic axial transmission velocity measurement on cortical bone models. J Acoust Soc Am 2004; 115: 2314-2324.

[20] Yablonovitch E. Inhibited spontaneous emission in solid-state physics and electronics. Phys Rev Lett 1987; 58: 2059-2062.

[21] John S. Strong localization of photons in certain disordered dielectric superlattices. Phys Rev Lett 1987; 58: 2486-2489.

[22] Lu MH, Feng L, Chen YF. Phononic crystals and acoustic metamaterials. Mater Today 2009; 12: 34-42.

[23] Notomi M, Yamada K, Shinya A, Takahashi J, Takahashi C, Yokohama I. Extremely large group-velocity dispersion of line-defect waveguides in photonic crystal slabs. Phys Rev Lett 2001; 87: 253902.

[24] Krauss TF. Slow light in photonic crystal waveguides. J Phys D Appl Phys 2007; 40: 2666-2670.

[25] Das S, Yin W. Trends in the global aluminum fabrication industry. JOM 2007; 59: 83-87.

[26] Hastings FD, Schneider JB, Broschat SL. Application of the perfectly matched layer (PML) absorbing boundary condition to elastic wave propagation. J Acoust Soc Am 1996; 100: 3061-3069.

[27] Chew WC, Liu QH. Perfectly matched layers for elastodynamics: a new absorbing boundary condition. J Comput Acoust 1996; 4: 341-359.

[28] Bossy E. SimSonic Suite User's Guide for SimSonic2D. 2012. http://www.simsonic.fr/downloads/SimSonic2D_UserGuide.pdf.

[29] McSkimin HJ. Velocity of sound in distilled water for the temperature range 20–75 C. J Acoust Soc Am 1965; 37: 325-328.

[30] Thomas JF Jr. Third-order elastic constants of aluminum. Phys Rev 1968; 175: 955.